Boreal and temperate snow cover variations induced by black carbon emissions in the middle of the 21st century

Ménégoz, M.[1], Krinner, G.[1], Balkanski, Y.[2], Cozic, A.[2], Boucher, O.[3], Ciais, P.[2].

[1] CNRS and UJF Grenoble 1, Laboratoire de Glaciologie et Géophysique de l'Environnement (LGGE, UMR5183), 38041 Grenoble, France.

[2] Laboratoire des Sciences du Climat et de l'Environnement, IPSL, CEA-CNRS-UVSQ, Gif-sur-Yvette, France.

[3] Laboratoire de Météorologie Dynamique, IPSL, Université P. et M. Curie, Paris, France.

Corresponding author: martin.menegoz@lgge.obs.ujf-grenoble.fr

Abstract

We used a coupled climate-chemistry model to quantify the impacts of aerosols on snow cover north of 30°N both for the present-day and for the middle of the 21st century. Black carbon (BC) deposition over continents induces a reduction in the Mean Number of Days With Snow at the Surface (MNDWS) that ranges from 0 to 10 days over large areas of Eurasia and Northern America for the present-day relative to the pre-industrial period. This is mainly due to BC deposition during the spring, a period of the year when the remaining of snow accumulated during the winter is exposed to both strong solar radiation and large amount of aerosol deposition induced themselves by a high level of transport of particles from polluted areas. North of 30°N, this deposition flux represents 222 Gg BC month^{-1} on average from April to June in our simulation. A large reduction in BC emissions is expected in the future in all of the Representative Concentration Pathway (RCP) scenarios. In particular, considering the RCP8.5 in our simulation leads to a decrease in the spring BC deposition down to 110 Gg month^{-1} in the 2050s. However, despite the reduction of the aerosol impact on snow, the MNDWS is strongly reduced by 2050, with a decrease ranging from 10 to 100 days from pre-industrial values over large parts of the Northern Hemisphere. This reduction is essentially due to temperature increase, which is quite strong in the RCP8.5 scenario in the absence of climate mitigation policies. Moreover, the projected sea-ice retreat in the next decades will open new routes for shipping in the Arctic. However, a large increase in shipping emissions in the Arctic by the mid 21st century does not lead to significant changes of BC deposition over snow-covered areas in our simulation. Therefore, the MNDWS is clearly not affected through snow darkening effects associated to these Arctic ship emissions. In an experiment without nudging toward atmospheric reanalyses, we simulated however some changes of the MNDWS considering such

aerosol ship emissions. These changes are generally not statistically significant in boreal continents, except in the Quebec and in the West Siberian plains, where they range between -5 and -10 days. They are induced both by radiative forcings of the aerosols when they are in the snow and in the atmosphere, and by all the atmospheric feedbacks. These experiments do not take into account the feedbacks induced by the interactions between ocean and atmosphere as they were conducted with prescribed sea surface temperatures. Climate change by the mid 21st century could also cause biomass burning activity (forest fires) to become more intense and occur earlier in the season. In an idealized scenario in which forest fires are 50% stronger and occur 2 weeks earlier and later than at present, we simulated an increase in spring BC deposition of 21 Gg BC month^{-1} over continents located north of 30°N. This BC deposition does not impact directly the snow cover through snow darkening effects. However, in an experiment considering all the aerosol forcings and atmospheric feedbacks, except those induced by the ocean-atmosphere interactions, enhanced fire activity induces a significant decrease of the MNDWS reaching a dozen of days in Quebec and in Eastern Siberia.

1 Introduction

The boreal regions have been characterized as a region very sensitive to climate change (Lemke et al., IPCC, chapter 4, 2007). One reason for the amplification in Arctic and Subarctic surface warming in response to increased greenhouse gas concentrations is the snow and sea-ice albedo feedback, which decreases surface albedo as snow and sea ice further melt and disappear in response to the warming by greenhouse gases (Serreze et al., 2006, Qu et al., 2007). Both sea-ice and snow-cover extents have been observed to shrink over the last decades in the Northern Hemisphere (Serreze et al., 2007, Shi et al. 2011). Snow-cover extent is expected to decrease further during the 21st century (e.g. Hosaka et al., 2005, Frei and Gong, 2005). However, it is quite difficult to evaluate accurately this decrease using climate models, because of both the complexity of the interactions between the snow and the atmosphere and the uncertainties when predicting future anthropogenic climate forcing (Qu and Hall, 2006 and 2007, Ghatak et al. 2010).

In contrast with the Antarctic, the Arctic atmosphere is quite polluted. An ensemble of short-lived species emitted in the industrialised mid-latitude regions of the Northern Hemisphere are transported towards the Arctic, where their lifetime increases due to the weak intensity of removal processes, in particular during the winter. The transport of pollutants into the Arctic atmosphere occurs especially in spring, and has been referred to cause the "Arctic Haze" phenomenon (e.g. Shaw, 1995, Stohl et al., 2006). Ozone and aerosols are the main short-lived species transported toward the Arctic that impact significantly the climate of this region, modifying regionally the radiative balance of the atmosphere (Law and Stohl, 2007). Ozone is a strong greenhouse gas, inducing a positive radiative forcing and causing a regional increase of the surface temperature (Shindell et al., 2006). Sulphate, Organic Carbon (OC) and nitrate aerosols are known to scatter solar radiation, inducing a negative radiative forcing at the top of the atmosphere and a cooling of the Earth's surface (Penner et al., 2001, Kanakidou, 2005). Black Carbon (BC) strongly absorbs solar radiation, inducing a positive forcing at the top of the atmosphere and a negative instantaneous forcing at the surface (Reddy et al., 2005). The heating of the atmosphere due to BC induces also an increase in the downward longwave radiation. Over highly reflective surfaces like snow covered areas, this increase in the longwave flux can be higher than the decrease of the shortwave flux induced by atmospheric BC (Quinn et al., 2008). In addition to these direct radiative forcings, aerosols affect clouds microphysics, processes referred to as the aerosol indirect effects. Although uncertain, these effects are thought to induce a negative radiative forcing, both at the top and the bottom of the troposphere (Lohmann et al., 2005). However, it has been suggested that there is also a longwave positive radiative forcing from aerosol-cloud interactions in the Arctic (Garrett and

Zhao, 2006; Lubin and Vogelmann, 2006). In addition, once deposited to snow or ice, BC and OC absorb radiation within the snowpack, and cause an earlier snow disappearance or decrease the snow mass, inducing a positive forcing at the surface, through decreased albedo (e.g. Warren and Wiscombe, 1980, Clarke and Noone, 1985, Jacobson, 2004, Hadley and Kirchstetter, 2012). Overall, Shindell and Faluvegi (2009) and Shindell (2012) pointed out that the temperature response to a radiative forcing is not necessarily correlated with the location of this radiative forcing. This is particularly true for the Arctic surface temperature response, which can be of opposite sign to that of the radiative forcing. This points to the necessity to apply Global Circulation Models (GCM) to quantify the surface temperature response to different radiative forcings in a particular region. Overall, Shindell (2007) and Shindell and Faluvegi (2009) estimate that both anthropogenic well-mixed greenhouses gases and short-lived species have contributed to the Arctic warming.

The main source of aerosol in the Arctic atmosphere is the transport from polluted regions in North America, Europe and Asia, while local aerosol emissions are very small (Shindell et al., 2008; Browse et al., 2012). Future aerosol concentrations in the Arctic are therefore very dependent on the evolution of the anthropogenic emissions from these regions. According to the Representative Concentration Pathway (RCP, Moss et al., 2008) emission scenarios, aerosol emissions in Northern America and Europe are estimated to have reached maximum values at different time periods during the 20^{th} century, depending on countries and on the chemical species under consideration (Bond et al. 2007, Smith et al., 2011). These regions now experience a significant decrease in their aerosol emissions. This is not the case of Asian emissions, which are still increasing. Their decrease is projected to take place in the next decades, although the exact timing is quite difficult to estimate, as the projections for energy demand, biofuel consumption and the introduction of new technologies are not set in stone (Ohara et al., 2007). In addition to anthropogenic emissions occurring in densely populated and industrialized regions, it seems that two local sources could affect the Arctic atmosphere in the decades to come: first, ship emissions could increase significantly, as summer sea-ice retreat will open new routes across the Arctic Ocean (Corbett et al. 2011). In particular, the possible increase of petroleum activities, extraction and refining, could induce an enhancement of ship traffic in some parts of the Arctic. However, the atmospheric pollution associated to such emissions in the Arctic should be limited by the decrease in emission factor as technology progresses (Peters et al., 2011); second, biomass burning emissions are expected to become stronger and to occur earlier in the season. The earlier occurrence of forest fires has recently been observed in high latitudes, in particular during warmer and dryer spring periods, in response to climate warming (e.g. Warneke et al. 2009). Flannigan et al. (2009a; 2009b) projected for instance that climate warming will induce an increase of fire activity in temperate and boreal regions, mainly from forest wildfires.

The goal of this study is to estimate the snow-cover variations in the boreal and temperate regions for the middle of the 21st century using simulations with a global coupled atmospheric general circulation and chemistry model prescribed with different aerosol local emission scenarios. As our quite coarse model is not able to describe realistically the seasonal snow cover over regions with complex topography, we excluded from our analysis most of the mountain ranges of the Northern Hemisphere. In particular, we excluded a large part of Himalaya, choosing a domain of study extended from 30°N to the North Pole. Using a land surface model enhanced for including the effects of BC on snow albedo, we investigate how the deposition of absorbing aerosols on snow affects snow cover dynamics and feedbacks on regional climate. We evaluate the snow-cover changes in the 2050 decade for the intensive RCP8.5 scenario (Representative Concentration Pathway 8.5, Moss et al., 2008, 2010, Riahi, 2007), and analyse thereafter the role of possible enhanced aerosols local emissions in the Arctic region.

2 Experimental set-up

2.1 Model description

We used the "LMDZ-INCA-ORCHIDEE" atmospheric General Circulation Model to study the interactions between atmosphere, aerosols and snow-covered areas. This model consists of three coupled modules: the LMDZ general circulation model represents the atmospheric component (Hourdin et al., 2006). INCA (Interactions between Chemistry and Aerosols) describes gas- and aqueous-phase chemistry (Hauglustaine et al., 2004 ; Boucher et al., 2002), as well as aerosol physical properties such as size and hygroscopicity (Balkanski et al., 2010), which control the amount of wet and dry deposition. The coupling between the LMDZ and INCA models allow for an interactive simulation of five aerosol chemical species, namely sulphate, BC, OC, sea-salt and dust. Direct aerosol forcing is taken into account for BC, OC, seasalt and dust, and both direct and indirect effect are taken into account for sulphate, BC and OC aerosol, as described in Déandreis et al. (2012). We used here LMDZ and INCA with a horizontal resolution of 96 x 95 grid points in longitude and latitude, and with a vertical discretisation of 19 layers. Finally the ORCHIDEE land surface model serves as the land surface boundary condition for LMDZ and describes exchanges of energy and water between the atmosphere, the soil and the biosphere (Krinner et al., 2005), including a dynamic snow module. The coupling between LMDz and ORCHIDEE is described by Hourdin et al. (2006), and those between LMDz and INCA is detailed by Hauglustaine et al. (2004) for chemistry and tracers and by Balkanski et al. (2007, 2010) and Déandreis et al. (2012) for the computation of the aerosols radiative forcings.

For this work, we used the detailed representation of snow-cover implemented in ORCHIDEE by Krinner et al. (2006) who studied the interactions between dust aerosol and ice-sheets in Northern Asia during the last glacial maximum (21000 years BP). In this scheme, snow albedo and snow cover are described separately for forests and grasslands/deserts, with a subgrid-scale orographic variability to compute accurately the energy balance in mountainous areas (Douville et al., 1995, Roesch et al., 2001). The aerosol content of the snow and its albedo are computed with a two-layer scheme, with a top layer of 8 mm (Snow Water Equivalent, SWE), and a bottom layer containing the remaining snow. A detailed description of the treatment of the snow/aerosol interactions in ORCHIDEE can be found in Krinner et al. (2006). However, only dry-deposited dust aerosol was taken into account in this study. Here, we also take into account BC, as its very absorbing property makes it likely to impact significantly the snowpack energy balance and the snow cover extent (e.g. Jacobson, 2004). Unfortunately, OC deposition on snow is not taken into account in our simulation. This aerosol also absorbs solar radiation, but there remain a lot of uncertainties concerning its radiative properties and its behaviour within the snowpack. We hope to take these processes into account in a further study. BC dry and wet depositions are computed by the INCA atmospheric chemistry module with a six-hourly time step. As in Krinner et al (2006), dry deposition contributes to increase the aerosol content in the top snow layer. Wet deposition also supplies aerosol to the surface layer, but it should be noted that this process is associated with an entry of fresh snow. If snowfall brings more snow than the maximum height of the snowpack surface layer, then aerosols in this previous surface layer are transferred into the bottom layer. Note that we considered a constant snow density of 330 kg m^{-3}. In further studies, we hope to include a more realistic representation of snow density in our model. If snowfall brings less than the maximum height of the surface layer, the new aerosol concentration of the surface layer is computed with the proportional contributions of the old aerosol concentration of the surface layer and those of the snowfall which reaches the surface layer (wet deposition). During melt or sublimation, snow mass is supposed to be lost from the surface layer. This one is therefore extended downwards to attain 8 mm SWE (if enough snow remains in the bottom layer). The aerosol mass corresponding to the lost snow height is added to those of the new surface layer. The timestep used to compute the snow aerosol content is the same as those applied to the whole surface scheme, *i.e.* 30 min. More details about this snow scheme can be found in Krinner et al. (2006). Conway et al. (1996) observed that BC could be flushed effectively trough the snow in melting conditions, with velocities strongly dependent on the particle size. However, the Conway et al. (1996) study was based upon experiments with particularly high rates of snow melting since they were performed during summer at altitudes around 2000 meters over the Northern United States. More recent observations by Aamaas et al. (2011) in Spitsbergen showed that BC aerosols tend to stay at the surface of the snowpack even during melting conditions. Building on this experimental evidence, and in contrast with Krinner et al. (2006), we will consider in this study that both dust and BC do not flush through the snow, and stay at the surface until a new snowfall occurs or until the disappearance of the snow-cover. This assumption could overestimate the magnitude of BC aerosol effects on the snow cover and climate.

Snow albedo is estimated using the parameterisation of Warren and Wiscombe (1980), which is adapted for snow containing aerosols. As in Krinner et al. (2006), the snow albedo of the bottom snowpack layer is computed first for diffuse radiation as a function of the underlying albedo, snow grain size and aerosol content. Snow grain size evolves prognostically as a function of snow age and temperature (Marshall and Oglesby, 1994), but unlike the aerosol content, it takes the same value in both snow layers. The spherical albedo of the bottom layer is then used as the underlying albedo for computing the albedo of the surface layer, both for diffuse and direct solar radiation. Snow albedo is averaged separately in the visible and near-infrared parts of the solar spectrum. We adopt the same aerosol physical properties as used in Balkanski et al. (2010) to evaluate their radiative forcings in the atmosphere. Within the snow, we do not know the extent to which aerosols are internally mixed, how they interact with snow grains, and how their hygroscopic and radiative properties evolve in time. Faced with all these uncertainties, we decided to consider simpler physical and radiative properties for aerosols in the snow in comparison with atmospheric aerosols. In futur model developments, we hope to include a more accurate representation of the interaction between aerosols and snow grain. Flanner et al. (2012) showed that accounting for the internal mixing of BC within snow grains increases its radiative forcing by 40 to 85% compared with treatments of externally-mixed BC in snow. Therefore, the simplification applied in our study may potentially underestimate the BC effect on snow albedo. The size and radiative parameters for dust are the same as used by Krinner et al (2006), following Guelle et al. (2000) and Balkanski et al. (2007). Black carbon is assumed to follow a log-normal size distribution with a median number radius of 11.8 nm, characteristic of freshly emitted soot (Dentener et al., 2006, Jacobson et al., 2004). In the real world, this diameter increases quickly, as BC undergoes ageing and coagulation and can be coated by other aerosols in the atmosphere. However, as we do not consider internal mixtures for BC in snow, we consider that BC aerosols regain their initial size when incorporated in the snowpack. We considered a BC density of 1 g cm^{-3}, and the refractive index for BC is taken to be m=1.75-0.45i. Refractive indices for ice are taken from the GEISA database (Jacquinet-Husson et al., 1999). The corresponding mass absorption cross-section (MAC) of BC resulting from these assumptions of size distribution, density, and refractive index reaches a value of 7.6 $m^2.g^{-1}$ at 545 nm (mid-visible, see the MAC definition of Bond and Bergrstrom, 2006, and Boucher, 2011). This value is comparable to 7.5 ±1.2 $m^2.g^{-1}$, a value found by Flanner et al (2007) and Bond and Bergrstrom (2006). Such value could however be reevaluated in further study, as Flanner et al.

(2012) found larger values considering internal mixing for snow and aerosol.

2.2 Description of simulations

Table 1 describes the eight 11-year global simulations that we performed to characterize the impact of BC deposition on snow cover both for the present period and for the middle of the 21^{st} century. We exclude from our analysis the first year of simulation, considered as a spin-up period. The two first experiments - designated as S1 and S1B - describe the present-day atmospheric state (1998-2008), using prescribed observed Sea Surface Temperature (SST, see Rayner et al., 2003) with winds nudged toward ERA-40 reanalysis from the European Centre for Medium-range Weather Forecasts (ECMWF). Note that pressure, temperature and humidity are computed with the LMDZ model without nudging in these experiments. The nudging is applied only for horizontal winds as described in Coindreau et al. (2006). Such protocol is very useful to reproduce the observed atmospheric state (Douville, 2010), letting however the model partially free to react to external forcings. We only applied the nudging to winds to avoid possible inconsistencies between winds and other meteorological variables (pressure, temperature, and moisture). These experiments were conducted with the present-day global aerosol emission inventory described in Lamarque et al. (2010), an inventory made for the Coupled Model Inter-comparison Project Phase 5 (CMIP5, CLIVAR special issue, 2011). In S1B, the BC content in the snow is set to zero, whereas it is computed from aerosol deposition in all the other experiments. The six other experiments were conducted over the period 2050-2060. They are based upon the aerosol and gases intensive emission scenario RCP8.5 (Representative Concentration Pathway 8.5, Moss et al., 2008, 2010, Riahi, 2007), characteristic of a scenario with no climate mitigation policies to limit greenhouse gas emissions. This scenario corresponds to a total anthropogenic forcing in 2100 of approximately 8.5 W m^{-2}. All six experiments were conducted with prescribed SST for the 2050s decade as produced from a previous coupled ocean-atmosphere simulation using IPSL-CM5A configuration in the context of the CMIP5 exercise (Dufresne et al., 2012). As for the two present-day simulations, using prescribed SST for these experiments cancel completely all the possible feedbacks involving the atmosphere ocean interactions. The first one of these six experiments – designated as S2 – has been performed with the aerosol emission inventory corresponding to that defined for the RCP8.5 scenario (Lamarque et al., 2009). Importantly, none of the RCP emission inventories used in CMIP5 simulations over the 21^{st} century considers variations of “local” emissions in the Arctic, which could be associated to a significant increase in ship traffic in the Arctic or to an intensification of biomass burning in boreal and temperate regions. For this reason, we performed another simulation – S3 – similar to S2 but replacing the baseline Arctic ship emissions in the RCP8.5 2050 by a scenario that includes important ship traffic over Arctic routes. These larger ship emissions are based on the “high-growth” scenario of Corbett et al. (2010), considering a high increase in ship traffic over the current Arctic routes. This scenario takes also into account the diversion routes opened during the summer following the seasonal retreat of sea-ice expected in the next decades. Finally an S4 simulation was also performed, similar to S2, but with enhanced biomass burning activity. Following Flannigan (2009a; 2009b), we consider an increase of 50% of BC and other aerosols emitted by fire during all the year. In addition, we consider also a 1-month extension of the fire season in the Northern hemisphere (starting 15 days prior and extending 15 days after the fire season of the present-day): From January to June (resp. from August to December), monthly emissions are computed as the average between the emission of the current month and those of the following (resp. previous) month. S3 and S4 emission variations are applied to sulphate, BC and OC. S2, S3 and S4 experiments consist of a pair of 11-years simulations, with initial conditions slightly modified in one of them, to be able to analyze 20 years of model output, as 10 years would clearly be insufficient to make comparisons statistically robust. In addition, to evaluate in more details the impact of the future aerosol emissions changes without considering atmospheric feedbacks, we realized three more experiments nudged toward our first 2050-2060 simulation: S2_N, S3_N and S4_N all have winds nudged toward S2, each of them using the same aerosol emissions as respectively S2, S3 and S4. Note that S2_N has been nudged toward itself (S2). This has been done to analyze the difference between simulations induced by the aerosol emissions change and not by the nudging itself.

Current BC emissions are particularly intense over the main industrialized regions of the Northern Hemisphere (Figure 1a) with 2878 Gg year^{-1} of BC emitted north of 30°N in the CMIP5 emission inventory (Lamarque et al., 2010) that we used for our S1 simulation. Regarding the difference between S2 and S1 (Figure 1b), we diagnose that according to the CMIP5 inventory, BC emissions are expected to significantly decrease over the major parts of industrialized areas in RCP8.5 (-1588 Gg year^{-1}), except in some regions of Central Asia. Note that this emission decrease is significant in all the RCP scenarios. These decreased aerosol emissions are projected by integrated assessment models under the hypothesis that increases in a country's wealth are accompanied with the introduction of new technologies to reduce emissions. Note that all the different RCP consider the same evolution for these technologies evolutions. This being said, the RCP8.5 projections indicate an increase of emissions over the oceans, associated to an increase in ship and air traffic, which appears inevitable (Eyring et al., 2005, Søvde et al., 2007). Figure 1c shows the increase in BC emissions estimated by Corbett et al. (2010) consequent to the evolution of ship traffic over the Arctic Ocean which could take place in addition to the RCP8.5 emissions for 2050. Note that we consider a diminution of shipping emissions for current routes, as Arctic new routes would partially replace current ones (Corbett et al., 2010). For this reason, the total difference in emissions with the

S2 simulation is very small (only +3.9 Gg year^{-1}). Finally we show in Figure 1d the increase in BC emissions associated to the idealized lengthening (+ 15 days before and between the fire season) and intensification (+50%) of biomass burning season applied on top of the RCP8.5 emission scenario (+ 236 Gg year^{-1} north of 30°N). Note that biomass burning emissions are assumed to be constant during all of the 21st century in the RCP8.5 scenario.

3 Results

We computed the Mean Number of Days per year With Snow at the surface (MNDWS) in all of our simulations as an indicator of the effects of aerosols emissions on snow cover. We considered the surface to be snow covered when the snow mass averaged over one day exceeds 0.01 kg.m^{-2} (i.e. 0.01 mm. snow water equivalent). Note that dust emissions were constant for all the simulations. In the following, we will not discuss the dust effects on snow. Figure 2a and 2b represent the MNDWS as observed (NSIDC, 2008) and modelled in our present-day control simulation S1, respectively. The MNDWS ranges from several days at 30°N to almost a complete year north of 75°N. The goal of our study is not to analyse in detail the ability of our GCM to describe the snow cover, as we will focus more on the analysis of sensitivity experiments with this GCM. Nevertheless, looking at the Root Mean Square Error (RMSE) between modelled and observed MNDWS (Figure 2c), we see that our model describes quite well the snow cover duration over flat areas (RMS varying between 5 and 20). This is not the case in mountainous areas like the Himalayas, the Altay Mountains, the Alps and the Rocky mountains where the RMSE generally exceeds values of 40 and can reach values of 300 days. As a consequence, we have to be very careful when we draw conclusions from the analysis of our simulation in these regions. Such huge errors are clearly due to the coarse resolution of our model, which does not allow a correct representation of the complex topography of these mountain ranges. Note that we did not consider the number of days with snow at the ground over glaciers, icecaps or sea ice in our study. We discarded as well snow cover variations modelled in grid-cells located just next to icecaps (Greenland) since the representation of these icecaps is also not accurate due to the coarse spatial resolution of our model.

In the following, we discuss the difference of MNDWS between our different simulations. The statistical significance was estimated using a two-sample t-test. This statistical test is applied to validate the hypothesis that the mean of two simulations are different at the 95% significance level. All areas with statistically significant differences are shaded in grey on Figures 3 to 7. Regarding present-day conditions, considering the influence of BC deposition on snow albedo induces a decrease of the MNDWS that is statistically significant over a major part of the continents of the Northern hemisphere (Figure 3a, difference S1-S1B). This decrease lies within a range of 1 to 10 days over large areas of Eurasia and Northern America. Regarding future conditions, there is a significant decrease of the MNDWS in the S2 simulation for 2050 (Figure 3b). This reduction is statistically significant, and ranges from 10 to 100 days in most parts of northern continental areas. Due to global warming forced by greenhouse gases, the beginning of the snow-accumulating season (respectively, the beginning of the snow-melting season) is modelled with ORCHIDEE coupled to LMDZ to occur later in autumn (resp. earlier in spring) in most snow-covered northern regions. A negative trend of MNDWS has already been observed during the last decades (e.g. Déry et al., 2007, Roesch et al., 2006, Mote et al., 2005). Moreover, Hosaka al. (2005) and Brutel-Vuilmet et al. (2012) expect an acceleration of this phenomenon into the 21st century. Similar to the results reported by Hosaka et al. (2005), we found that the snow cover changes are also driven in the model by snowfall variations. As an example, the snow cover duration is less reduced in Eastern Siberia than in Scandinavia, because snowfall is modelled to increase in Eastern Siberia in the middle of the 21st century. We found also a slight increase of the MNDWS compared to present-day over some northern parts of China and over the USA, also induced by a local increase in snowfall for the modelled LMDZ climate in 2050. However, we have to be very careful with this last result, as it concerns mountainous areas, where the GCM coarse resolution cannot provide accurate results as explained above.

Considering an increase in aerosol emissions from Arctic ships or from biomass burning in our 2050-2060 nudged experiment induce MNDWS variations quasi equal to zero (see Figure 3c and 3d, showing respectively MNDWS differences S3_N-S2_N and S4_N-S2_N). It clearly means that the snow albedo changes associated with this possible increase in aerosol emission is negligible in comparison with the snow albedo changes induced today by the current aerosol emissions in the Northern Hemisphere. We have to keep in mind that these future sensitivity experiments were nudged, a process that limits atmospheric feedbacks: these experiments allow to quantify the changes of snow cover duration induced by the aerosol effects on snow albedo, strongly minimizing both the effect of aerosols when they are in the atmosphere and the temperature changes induced by the snow cover variations. The nudging was applied only to the horizontal wind, but temperature is also indirectly nudged as these two variables are quite dependent in a hydrostatic approximation model (e.g. Holton, 2004). Hence, the variations of temperature induced by atmospheric aerosols changes are partially cancelled in these nudged simulations. Nevertheless, the effect of atmospheric aerosol was not completely inactivated in these nudged simulations, as it induces also a modification of the radiative flux reaching the surface and a residual atmospheric warming. The complete effect of aerosols can be evaluated through simulations performed without nudging, as it was done for experiments S3 (with an increase in arctic ship traffic) and S4 (with an increase in biomass burning emissions). Nevertheless, we have to keep in mind that all of these future experiments used the same prescribed SST, which cancel the feedbacks which could be generated through interactions with the ocean. Since our study focuses on the continental response to a continental forcing, the analysis presented here should not be too much affected. Figures 4a and 4b show that without nudging the variations in MNDWS with enhanced ship and fire emissions can be positive or negative depending upon the region. They are spatially variable, and reach values ranging from -10 to +10 days per year in comparison with our 2050-2060 simulation performed with the standard RCP aerosol emissions (S2). Note that these variations of MNDWS are not statistically significant according to our two-sample t-test over the major part of the Northern hemisphere. In other words, it means that the signal induced by the changes of aerosol emissions is too low to affect the highly variable coupled land-atmosphere system. Nevertheless, we obtained a statistically significant decrease of MNDWS in Quebec and in Siberia, both in simulation S3 and S4. These MNDWS local decreases reach 10 days averaged over the decade-long simulation of the 2050s.

4 Discussion

From the analysis of our nudged and not nudged experiments, we estimate that the possible increase in aerosol emissions from ships or boreal fires will not affect significantly the snow cover directly from snow darkening effects. However, this conclusion may not hold if we had also accounted for the atmospheric effects of aerosols. These effects are however very difficult to quantify: Shindell and Faluvegi (2009) showed that the patterns of temperature response and aerosol radiative forcing do not correspond on a regional basis. The difficulty to answer these complex questions is reinforced by the fact that ships emit different aerosol species (Balkanski et al., 2010), which have differentiated impacts on the climate system: They emit BC, an aerosol which absorbs solar radiation, warming its environment, but they also emit large amount of sulphate, an aerosol which strongly scatter solar radiation, cooling locally the atmosphere via direct end indirect effects (Lohmann, 2005). The sign of the radiative forcing induced by biomass burning, which also emits both BC, OC and sulphate depends also on the height at which the particles are transported (Abel et al., 2005). In front of all these complex questions, we discuss in the following when and how the MNDWS can be affected by increased ship and biomass burning aerosol emissions.

Both the scenario with enhanced biomass burning emissions and those with increased Arctic ship traffic emissions produce very low emissions in winter. In summer, the Northern Hemisphere experiences a reduced snow cover. During fall, when solar radiation is considerably reduced compared to summer, both atmospheric aerosols and aerosols deposited on snow surface have a weak impact on snow cover (Flanner et al., 2009). Spring is the season when the Arctic atmosphere experiences the most pollution (e.g. Shaw et al., 1995, Ménégoz et al., 2012). For all of these reasons, although summer is the period when aerosol concentrations from ship traffic and biomass burning are the largest, it is during the spring that we find the largest significant MNDWS changes associated to aerosol emissions considered in experiments S3 and S4 (Note that the MNDWS changes are very low in our simulation during the other seasons, not shown). The significant spring aerosol emissions are simultaneous with large residual snow cover over continental regions of the Northern Hemisphere, and thus have the potential to amplify regional warming. This is why we focus the following analysis on the interactions between snow and aerosols during the spring season (April-May-June).

4.1 BC deposition on snow

Present-day modelled BC spring deposition reaches 50 mg m^{-2} $month^{-1}$ in Europe and Northern America, and exceeds 100 mg m^{-2} $month^{-1}$ over South-east Asia (Figure 5a). Typical deposition values modelled in the pan-Arctic continental area (North of 60°N) range between 0.1 and 10 mg m^{-2} $month^{-1}$. In simulation S2, a drastic decrease in BC deposition is obtained over the whole Northern hemisphere for 2050 (Figure 5b), with the exception of central Asia and Alaska. In these regions, the anthropogenic emissions are increasing in the RCP8.5 scenario compared to current level (see Figure 1b). On average over all the continental surfaces of the Northern hemisphere, this decrease represents half of the present-day spring deposition (decrease of 110 Gg $month^{-1}$ for a present-day total of 222 Gg $month^{-1}$, north of 30°N). The simulation performed with extra high ship emissions in the Arctic (S3) does not induce significant changes of BC deposition in spring (Figure 5c) in comparison to the S2 2050 simulation. This is due to the fact that the additional Arctic ship emissions are mainly enhanced in summer, when ships use alternate Arctic routes. Yet, these enhanced ship emissions modify the atmospheric circulation and precipitation via the atmospheric aerosol radiative forcings in our sensitivity experiment. These changes are certainly responsible for the modelled spatial variations of aerosol deposition during springtime. Note that this very weak signal is not statistically significant, indicating that the increase of ships emissions only generated "noise" in the aerosol spring deposition signal of our sensitivity experiment S3. Such response can be therefore mainly explained by natural variability. By contrast with S3, the earlier fire season considered in simulation S4 causes a significant increase in BC spring deposition over both North America and North Asia (Figure 5d). The total increase of BC continental deposition in the S4 simulation represents 21 Gg $month^{-1}$. Regarding spring aerosol deposition, we can conclude that the MNDWS changes modelled in the S3 experiment is clearly not induced by snow darkening effects by aerosols. They are more due to aerosols when they are in the atmosphere, and to all the possible associated atmospheric feedbacks. Regarding S4 spring aerosol deposition, it is possible that snow darkening effect of BC have impacted the MNDWS via atmospheric feedbacks.

4.2 Spring Snow Water Equivalent (SWE)

During the spring, the present-day SWE ranges from 500 to 2000 mm in mountainous areas such as the Rocky Mountains, the Scandinavian mountains, the Ural Mountains or over Kamchatka (Figure 6a). Elsewhere, over high latitudes continental areas, it takes values on the order of 100 mm. Considering BC deposition on snow in the present-day conditions (S1 – S1B) induces only a small SWE decrease over large part of Eurasia an Northern America ranging from 0 to 10 mm (Figure 6b). However, in a few locations of Western America and Scandinavia, this decrease takes larger values, exceeding 100 mm. The strongest BC induced decrease in present-day SWE appears in regions where the SWE is generally elevated in spring. Overall, spring SWE is modelled to be much lower in the RCP8.5 2050 scenario than under present-day conditions, and the modelled SWE decrease reaches up to 50% over the major part of snow-covered areas (Figure 6c). There are very few regions where spring SWE is modelled to increase in S2 compared to S1, and these exceptions are North Eastern Canadian Islands, the Himalayan region and small parts of Northern Eurasia. An enhancement of ship traffic in the Arctic is predicted to induce an extra decrease of the SWE in Alaska, in the Canadian shield, and in large parts of Northern Eurasia, ranging from 10 to 100 mm (Figure 6d), and in the Baffin Island, reaching 10 mm. In the scenario S4 with an earlier spring biomass burning activity, spring SWE is modelled to decrease in many parts of the continental pan-Arctic areas, by up to 50 mm, except in Baffin Island and in very small regions of Northern Eurasia (Figure 6e). However, these modelled extra SWE changes in simulations S3 and S4 are not statistically significant according to a two-sample t-test, indicating that the signal of the local aerosol emissions taken into account is difficult to be characterized given the large amount of natural climate variability, and the fact that local emissions play a second order role (S3-S2 and S4-S2) compared to the fist order effect of GHG forced future warming effects on SWE (S2-S1).

The present-day SWE decrease induced by aerosol deposition is quite smaller than the decrease modelled in 2050 under the RCP8.5 scenario (see Figures 6b and 6c). The decrease of SWE expected in 2050 is due to the temperature increase associated with the greenhouse gas radiative forcing. This result clearly shows that the drastic reduction of BC deposition in the Northern Hemisphere in 2050 (Figure 5b) is clearly not sufficient to counteract the decrease of SWE induced by greenhouse gas radiative forcing and its associated temperature increase (Figure 6c). As explained previously, there are almost no changes in aerosol spring deposition in the simulation S3 with enhanced ship emissions. The modelled changes in MNDWS and SWE are therefore due to atmospheric aerosol effects, which can experience atmospheric feedbacks. For the S4 simulation with enhanced biomass burning in spring, there is a significant increase of aerosol deposition, which may explain a part of the MNDWS and SWE diminutions in some regions of Northern Eurasia and Northern America. This assumption appears very likely where the MNDWS variations are statistically significant, in North-eastern America as in central and eastern Siberia. However, the SWE variations are generally not statistically significant, and there is no clear correlation between BC deposition and snow cover variations. Therefore, it is likely that part of the SWE changes is also consecutive to surface energy balance changes or to snowfall variations in our simulations.

4.3 Spring snowfalls

Present-day spring snowfalls are widespread over a large part of the Northern hemisphere continents (Figure 7a). In our present-day simulation, the snow albedo decrease induced by BC aerosol deposition leads to a slight but statistically significant snowfall reduction (Figure 7b). A large part of the spring decrease in SWE between 2050 and present-day simulations (Figure 6c) can be explained by this snowfall feedback (Figure 7c). In most part of the spring snow-covered area of the Northern hemisphere, snowfall decreases by 50% (see Figure 7a and 7c) in S2 compared to S1. This is mainly due to temperature rise, which transforms snowfall into rainfall. We find only few and small areas, like North Eastern Canadian Islands, parts of the Himalayan region and very small parts of Northern Eurasia where snowfall increases. However, these increases may explain the SWE increases modelled in the same regions.

Based upon the sensitivity experiments S2, S3 and S4, we are able to evaluate the impact of an aerosol emission change in a 2050 scenario. In simulations S3, the spring SWE change exhibits a pattern similar to snowfall change in many continental areas of the Northern hemisphere, with a general decrease in the pan-arctic area, except in small areas like Baffin Islands and other Northern Canadian islands (Figure 7d). Therefore, we can assess that the atmospheric perturbations induced by enhanced ship traffic BC emissions in the Arctic induce a small decrease of snowfall over large area of the boreal continents. Even if these variations are not statistically significant according to a two-sample t-test, they partly contribute to the decrease of SWE modelled in the same region. However, it is very difficult to estimate which physical processes link snowfall variations to BC aerosol emissions change, since aerosols from ships contain both absorbing and reflective species which have complex interactions with the atmosphere (Balkanski et al., 2010). Regarding the S4 simulation, we can also assess that the snowfall decreases which take place in the major part of Northern America, in North-Eastern Europe and in North-east Asia (Figure 7e) are responsible for part of the modelled decrease of both MNDWS and SWE in these regions. However, this assumption is not verified in Northern Central Siberia, where we modelled an increase of snowfall but a decrease of the SWE and the MNDWS. In this region, the SWE decline is certainly induced by an aerosol forcing. It may be due both to a decrease of the snow albedo via aerosol deposition, and to a warming of the atmosphere associated to an increase in the atmospheric concentration of BC.

5 Conclusion

The snow-cover changes induced by aerosol emissions were evaluated in the boreal continental area both for the present-day and for the middle of the 21^{st} century. The following eight experiments were carried out: two present-day simulations, with one of them not considering the snow albedo variations induced by aerosol deposition, and six 2050-2060 simulations based upon the RCP8.5 gas and aerosol anthropogenic emission inventory.

We estimate that current aerosol emissions directly cause a decrease of the MNDWS ranging between 0 and 10 days in large areas of the boreal region. This "snow darkening effect" is essentially due to the BC deposition during the spring, a period of the year when the remaining of snow accumulated during the winter is exposed to both strong solar radiation and large amount of aerosol deposition. This deposition over continents represents 222 Gg $month^{-1}$ of BC north of 30°N. Recent papers have shown that the "snow darkening effect" affect as much the present-day snow cover as the warming induced by anthropogenic GHG (e.g. Flanner et al., 2007, 2009, 2012, Jacobson et al.2004).

The projected drastic decrease of the anthropogenic aerosol emissions from the RCP scenarios for the middle of the 21^{st} century in the Northern hemisphere may limit the decrease of snow albedo due to absorbing aerosol deposition. But this response is very much dependent on the quality of the emission scenarios, as no inflexion in BC emissions over Asia has been observed in the past decades. Nonetheless, a major part of snow-cover in the Northern hemisphere will experience a significant reduction under the GHG forced warming. By comparison with present-day conditions, the MNDWS was found to be reduced by 10 to 100 days over the major part of the continental regions of the Northern Hemisphere by the middle of the 21^{st}century. The main cause for this decrease is a temperature rise that substitutes snow to rain over several regions and accelerates melting. The relative contribution of the snow darkening effect to the total snow cover reduction will clearly decrease in the next decades, as those of the GHG forcing is expected to strongly increase. These conclusions have been reached with a future scenario that considers strong increases in greenhouse gases concentrations. The decrease of the aerosol impact on snow-cover should be relatively more important for a scenario with lower greenhouse gases concentrations.

Considering a significant additional increase in ship traffic in the Arctic by the mid 21^{st} century does not lead to significant changes of the aerosol deposition over snow-covered areas in the most sensitive period for a positive climate feedback, springtime. Therefore, the MNDWS is clearly not affected by snow darkening effects associated to these Arctic ship emissions. This result has been demonstrated using a simulation nudged toward the observed atmosphere, to quantify how aerosol deposition could affect directly the snow cover. We have to keep in mind that applying nudging techniques in these sensitivity experiments strongly limits all the possible atmospheric feedbacks, but does not cancel completely the diming happening in surface and the atmospheric warming due to atmospheric aerosols. As a consequence, atmospheric BC aerosols associated to these Arctic ships traffic have also no direct impact on the snow cover. In an experiment considering such an increase of ship emissions without nudging toward atmospheric reanalyses, we simulated some changes of the MNDWS. Ships emit absorbing aerosols like BC and to a lesser extent OC, but in comparison a lot more sulphur dioxide, which strongly scatters the incoming solar radiation, thereby cooling the atmosphere. Modifying the atmospheric energy balance by accounting for these aerosols affects the atmospheric circulation and the precipitation pattern. In this experiment, the MNDWS changes are generally not statistically significant in boreal continents, except in the Quebec and in the West Siberian plains, where the MNDWS decrease from 5 to 10 days.

Biomass burning activity proportionally emits more BC and OC aerosol and much less sulphate compared with ship traffic. We modelled a significant increase in BC spring deposition that exceeds 1 mg m^{-2} $month^{-1}$ over large parts of America and Eurasia in a 2050-2060 simulation that take into account forest fires that are 50% stronger and are projected to occur 2 weeks earlier and later than at present. This increase of BC spring deposition represents 21 Gg $month^{-1}$ on continents located north of 30°N. However, with such emissions, we do not simulate a reduction of the MNDWS in an experiment performed with winds nudged toward atmospheric reanalyses. This demonstrates that our biomass burning emission scenario does not induce a significant reduction of the snow cover, either via “snow darkening effects”, either via “aerosol diming”, and either via “atmospheric warming due to absorbing aerosols”. However, considering all the aerosol forcings and atmospheric feedbacks in an experiment performed without nudging, enhanced fire activity induces a significant decrease of the MNDWS reaching a dozen of days in Quebec and in Eastern Siberia.

Due to the snow-albedo feedback, the Arctic is a region very sensitive to climate change. As a consequence of this feedback, Flanner et al. (2009) showed that absorbing aerosol emissions reduced the springtime snow cover as much as anthropogenic greenhouse gases since the pre-industrial period. Consequently, limiting aerosol emissions appears as essential as limiting greenhouse gases emissions to slowdown the snow cover decline observed over the Northern Hemisphere. Foreseeing the possible emissions scenarios in the 21^{st} century, one can envisage for strong aerosol reductions in most industrialized region over the Northern Hemisphere with the introduction of advanced technologies in controlling emissions. However, increases in the emissions and concentrations of greenhouse gases that are projected in most scenarios are expected to significantly reduce the snow cover in the middle of the 21^{st} century. It appears very challenging to estimate accurately the snow cover changes induced by the possible changes in aerosol emissions in the Arctic and in the boreal region because of the complex processes linking aerosol forcing, atmosphere response and snow cover dynamics. Thanks to the comparison between our nudged and not nudged simulations, we can maintain that the decrease of MNDWS that we simulated in our scenario with increased ships traffic or enhanced fire emissions is more explained by the atmospheric feedbacks than by the forcing directly generated by these aerosols, either in the atmosphere, either deposited on the snow. The aerosol forcing is the initiator of the modelled changes, but several feedbacks can be involved: As an example, a warming induced by absorbing aerosols located in the snow or in the atmosphere will generate a diminution of snow cover. This one will induces a diminution of the surface albedo, therefore an increase of the solar energy absorbed by the surface, and finally an increase of temperature, itself impacting the atmospheric circulation and the precipitation pattern and phase. In particular, we found in our simulation a diminution of both snowfall and SWE in the area where we modelled a decrease of MNDWS. Such variations are associated to a warming of the low layers of the atmosphere in these regions (not shown). Further simulations could be performed to diagnose accurately the aerosol direct and indirect effects generated by the aerosol emissions scenarios that we suggest in this paper. Such protocol has yet been applied to estimate the radiative forcing of the present-day aerosol emissions (IPCC, 2007). However, if it is quite easy to apply this protocol for the aerosol direct effect (e.g. Balkanski et al., 2010), it appears to be a more delicate exercise for indirect effects (e.g. Déandreis et al., 2012). Besides, the snow albedo variations induced by absorbing aerosol deposition is quite dependent on the chemical composition of these aerosols (Wang et al., 2012), their evolution within the snow cover (Aamas et al., 2011, Conway et al., 1996), and their mixing state with snow grains (Flanner et al., 2012). Further experiments dealing with these processes could provide a realistic spread about the existing knowledge concerning BC and its interactions with snow albedo. Anyway, we predict that the likely future aerosol emissions from ships traffic over the Arctic region or an increase in biomass burning will play a minor role in the reduction of continental snow cover area trough snow darkening direct effects at high Northern latitudes. We have not attempted to predict future changes in sea ice due to these effects but these may be significant.

Acknowledgements

This work was supported by Agence Nationale de la Recherche under contract ANR-09-CEP-005-02/PAPRIKA and by funding from the European Union 7th Framework Programme under project LIFE SNOWCARBO. We would like to thank the “Commissariat à l’Energie Atomique et aux Energies Alternatives” and GENCI for providing computer time for the simulations presented in this paper. The figures have been prepared with Ferret free software. We thank J. J. Corbett for providing ship traffic emissions scenarios in the Arctic, and the National Snow and Ice Data Centre (NSIDC, Boulder, CO) for providing IMS daily Northern Hemisphere snow and ice analysis. We thank the editor and the 4 anonymous reviewers for their relevant comments, which helped to refine our study and to improve the manuscript.

References

Aamaas, B., Bøggild, C.E., Stordal, F., Berntsen, T., Holmén, K., Ström, J.: Elemental carbon deposition to Svalbard snow from Norwegian settlements and lonb-range transport, Tellus 63B, 340–351, 2011.

Abel, S. J., Highwood, E. J., Haywood, J. M., and Stringer, M. A.: The direct radiative effect of biomass burning aerosols over southern Africa, Atmos. Chem. Phys., 5, 1999-2018, doi:10.5194/acp-5-1999-2005, 2005.

Balkanski, Y., Myhre, G., Gauss, M., Rädel, G., Highwood, E. J., and Shine, K. P.: Direct radiative effect of aerosols emitted by transport: from road, shipping and aviation, Atmos. Chem. Phys., 10, 4477-4489, 2010.

Balkanski, Y., M. Schulz, T. Claquin And O. Boucher, Reevaluation of mineral aerosol radiative forcings suggests a better agreement with satellite and AERONET data, Atmos. Chem. Phys., 7, 81-95, 2007.

Bond, T. C., E. Bhardwaj, R. Dong, R. Jogani, S. Jung, C. Roden, D. G. Streets, and N. M. Trautmann: Historical emissions of black and organic carbon aerosol from energy-related combustion, 1850 – 2000, Global Biogeochem. Cycles, 21, GB2018, doi:10.1029/2006GB002840, 2007.

Bond, T.C. & Bergstrom, R.W.: Light Absorption by Carbonaceous Particles: An Investigative Review, Aerosol Science and Technology, 40:1, 27-67, 2006.

Boucher, Olivier: *Aérosols atmosphériques, propriétés et impacts climatiques*, ed. Springer, 248 pp., 2011.

Boucher, O., Pham, M., Venkataraman, C.: Simulation of the atmospheric sulfur cycle in the Laboratoire de Météorologie Dynamique General Circulation Model. Model Description, Model Evaluation, and Global and European Budgets, Note n°23, IPSL, 2002.

Browse, J., Carslaw, K. S., Arnold, S. R., Pringle, K., and Boucher, O.: The scavenging processes controlling the seasonal cycle in Arctic sulphate and black carbon aerosol, Atmos. Chem. Phys., 12, 6775-6798, doi:10.5194/acp-12-6775-2012, 2012.

Brutel-Vuilmet, C., Ménégoz, M., and Krinner, G.: An analysis of present and future seasonal Northern Hemisphere land snow cover simulated by CMIP5 coupled climate models, The Cryosphere Discuss., 6, 3317-3348, doi:10.5194/tcd-6-3317-2012, 2012.

Conway, H., A. Gades, and C. F. Raymond: Albedo of dirty snow during conditions of melt, Water Resour. Res., 32(6), 1713–1718, doi:10.1029/96WR00712, 1996.

Clarke, A. D. and Noone, K. J.: Soot in the Arctic snowpack: A cause for perturbations in radiative transfer, Atmos. Environ., 19, 2045–2053, 1985.

Coindreau, O., Hourdin, F., Haffelin, M., Mathieu, A., Rio, C.: Assessment of physical parameterizations using a global climate model with strechable grid and nudging, Monthly Weather Review, 135:1474-1489, 2006.

Corbett, J. J., Lack, D. A., Winebrake, J. J., Harder, S., Silberman, J. A., and Gold, M.: Arctic shipping emissions inventories and future scenarios, Atmos. Chem. Phys., 10, 9689-9704, doi:10.5194/acp-10-9689-2010, 2010.

Déandreis, C., Balkanski, Y., Dufresne, J. L., and Cozic, A.: Radiative forcing estimates of sulfate aerosol in coupled climate-chemistry models with emphasis on the role of the temporal variability, Atmos. Chem. Phys., 12, 5583-5602, doi:10.5194/acp-12-5583-2012, 2012.

Dentener, F., Kinne, S., Bond, T., Boucher, O., Cofala, J., Generoso, S., Ginoux, P., Gong, S., Hoelzemann, J. J., Ito, A., Marelli, L., Penner, J. E., Putaud, J.-P., Textor, C., Schulz, M., van der Werf, G. R., and Wilson, J.: Emissions of primary aerosol and precursor gases in the years 2000 and 1750 prescribed data-sets for AeroCom, Atmos. Chem. Phys., 6, 4321-4344, doi:10.5194/acp-6-4321-2006, 2006.

Déry, S. J., and R. D. Brown: Recent Northern Hemisphere snow cover extent trends and implications for the snow-albedo feedback, Geophys. Res. Lett., 34, L22504, doi:10.1029/2007GL031474, 2007.

Douville, H., Royer, J.-F. and Mahfouf, J.-F.: A new snow parametrization for the Météo-France climate model. Part II: Validation in a 3-D GCM experiments, Clim. Dyn. 12, 37-52, 1995.

Dufresne J.-L., Foujols, M.-A., Denvil, S., Caubel, A. Marti, O., Aumont, O., Balkanski, Y., Bekki, S., Bellenger, H., Benshila, R., Bony, S., Bopp, L., Braconnot, P., Brockmann, P., Cadule, P., Cheruy, F., Codron, F., Cozic, A., Cugnet, D., de Noblet, N., Duvel, J.-P., Ethé, C., Fairhead, L., Fichefet, T., Flavoni, S., Friedlingstein, P., Grandpeix, J.-Y., Guez, L., Guilyardi, E., Hauglustaine, D., Hourdin, F., Idelkadi, A., Ghattas, J., Joussaume, S., Kageyama, M., Krinner, G., Labetoulle, S., Lahellec, A., Lefebvre, M.-P., Lefevre, F., Levy, C., Li, Z. X., Lloyd, J., Lott, F., Madec, G., Mancip, M., Marchand, M., Masson, S., Meurdesoif, Y., Mignot, J., Musat, I., Parouty, S., Polcher, J., Rio, C., Schulz, M., Swingedouw, D., Szopa, S., Talandier, C., Terray, P., Viovy, N.: Climate change projections using the IPSL-CM5 Earth System Model: from CMIP3 to CMIP5, Clim. Dyn., Special Issue, xxx-yyy, 2012.

Eyring, V., H. W. Kohler, A. Lauer, and B. Lemper: Emissions from international shipping: 2. Impact of future technologies on scenarios until 2050, J. Geophys. Res., 110, D17306, doi:10.1029/2004JD005620, 2005.

Flanner, M. G., Liu, X., Zhou, C., Penner, J. E., and Jiao, C.: Enhanced solar energy absorption by internally-mixed black carbon in snow grains, Atmos. Chem. Phys., 12, 4699-4721, doi:10.5194/acp-12-4699-2012, 2012.

Flanner, M. G., C. S. Zender, P. G. Hess, N. M. Mahowald, T. H. Painter, V. Ramanathan, and P. J. Rasch: Springtime warming and reduced snow cover from carbonaceous particles, Atmos. Chem. Phys., 9, 2481-2497, 2009.

Flannigan, M.D., Krawchuk, M.A., de Groot, W.J., Wotton, B.M. and Gowman, L.M.: Implications of changing climate for global wildland fire. International Journal of Wildland Fire,18, 483-507, 2009.

Flannigan, M.D., Stocks, B.J., Turetsky, M.R. and Wotton, B.M.: Impact of climate change on fire activity and fire management in the circumboreal forest. Global Change Biology, 15: 549-560. DOI: 10.1111/j.1365-2486.2008.01660.x, 2009.

Frei, A. and G. Gong: Decadal to Century Scale Trends in North American Snow Extent in Coupled Atmosphere-Ocean General Circulation Models. Geophysical Research Letters, 32:L18502, doi: 10.1029/2005GL023394, 2005.

Garrett, T. J. and C. Zhao: Increased Arctic cloud longwave emissivity associated with pollution from mid-latitudes. Nature, 440, 10.1038/nature04636, 787-789, 2006.

Ghatak, D., A. Frei, G. Gong, J. Stroeve, and D. Robinson: On the emergence of an Arctic amplification signal in terrestrial Arctic snow extent, J. Geophys. Res., 115, D24105, doi:10.1029/2010JD014007, 2010.

Guelle, W., Balkanski, Y., Schulz, M., Marticorena, B., Bergametti, G., Moulin, C., Arimoto, R., Perry, K.D.: Modelling the atmospheric distribution of mineral aerosol: comparison with ground measurements and satellite observations for yearly and synoptic time scales over the North Atlantic. J. Geophys Res 105:1997–2005, 2000.

Hauglustaine, D.A., Hourdin, F., Jourdain, L., Filiberti, M.A., Walters, S., Lamarque, J.F. and Holland, E.A.: Interactive chemistry in the Laboratoire de Météorologie Dynamique general circulation model : Description and background tropospheric chemistry evaluation, J. Geophys. Res. 109, 10.1029/2003JD003957, 2004.

Hadley, O.L., Kirchstetter, T.W.: Black carbon snow albedo reduction, Nature Climate Change, doi: 10.1038/NCLIMATE1433, 2012.

Holton, J. *R.: An Introduction to Dynamic Meteorology. New York: Academic Press, 2004.*

Hosaka, M., D. Nohara, and A. Kitoh: Changes in snow coverage and snow water equivalent due to global warming simulated by a 20km-mesh global atmospheric model. Scientific Online Letters on the Atmosphere, 1, 93–96, 2005.

Hourdin, F., and Coauthors: The LMDZ4 general circulation model: Climate performance and sensitivity to parametrized physics with emphasis on tropical convection. Climate Dyn., 27, 787–813, 2006.

Intergovernmental Panel on Climate Change (2007), Climate Change. The scientific Basis, Cambridge Univ. Press, Cambridge, U. K., 2007.

Jacobson, M.Z.: Climate response of fossil fuel and biofuel soot, accounting for soot's feedback to snow and sea ice albedo and emissivity. J. Geophys. Res., 109, D21201, 2004.

Jacquinet-Husson, N., Arié, E., Ballard, J., Barbe, A., Bjoraker, G., Bonnet, B. and Brown, L. R.: The 1997 spectroscopic GEISA databank. J Quant Spect Radiat Transfer 61:425–438, 1999.

Kanakidou, M., Seinfeld, J. H., Pandis, S. N., Barnes, I., Dentener, F. J., Facchini, M. C., Van Dingenen, R., Ervens, B., Nenes, A., Nielsen, C. J., Swietlicki, E., Putaud, J. P., Balkanski, Y., Fuzzi, S., Horth, J., Moortgat, G. K., Winterhalter, R., Myhre, C. E. L., Tsigaridis, K., Vignati, E., Stephanou, E. G., and Wilson, J.: Organic aerosol and global climate modelling: a review, Atmos. Chem. Phys., 5, 1053-1123, doi:10.5194/acp-5-1053-2005, 2005.

Koch, D., Schulz, M., Kinne, S., McNaughton, C., Spackman, J. R., Balkanski, Y., Bauer, S., Berntsen, T., Bond, T. C., Boucher, O., Chin, M., Clarke, A., De Luca, N., Dentener, F., Diehl, T., Dubovik, O., Easter, R., Fahey, D. W., Feichter, J., Fillmore, D., Freitag, S., Ghan, S., Ginoux, P., Gong, S., Horowitz, L., Iversen, T., Kirkevåg, A., Klimont, Z., Kondo, Y., Krol, M., Liu, X., Miller, R., Montanaro, V., Moteki, N., Myhre, G., Penner, J. E., Perlwitz, J., Pitari, G., Reddy, S., Sahu, L., Sakamoto, H., Schuster, G., Schwarz, J. P., Seland, Ø., Stier, P., Takegawa, N., Takemura, T., Textor, C., van Aardenne, J. A., and Zhao, Y. 2009. Evaluation of black carbon estimations in global aerosol models. Atmos. Chem. Phys., 9, 9001-9026, doi:10.5194/acp-9-9001-2009.

Krinner, G., Viovy, N., de Noblet-Ducoudre, N., Ogee, J., Polcher, J., Friedlingstein, P., Ciais, P., Sitch, S. and Prentice, IC.: A dynamic global vegetation model for studies of the coupled atmosphere-biosphere system. Glob. Biogeochem. Cycle, 19(1), 44 pp, 2005.

Krinner, G., O. Boucher and Y. Balkanski: Ice-free glacial northern Asia due to dust deposition on snow. Clim. Dyn., 27(6), 613–625, 2006.

Lamarque, J-F., Granier, C., Bond, T., Eyrling, V., Heil, A., Kainuma, M., Lee, D., Liousse, C., Mieville, A., Riahi, K., Schultz, M., Sith, S., Stehfest, E., Stevenson, D., Thomson, A., vanAardenne, J., and D. vanVuuren: Gridded emissions in support of IPCC AR5. IGAC Newsl. 41, 12–18, 2009.

Law, K.S. and Stohl, A.: Arctic Air Pollution: Origins and Impacts, Science*, 315 (5818), 1537-1540, doi:10.1126/science.1137695, 16 March 2007.*

Lamarque, J.-F., Bond, T. C., Eyring, V., Granier, C., Heil, A., Klimont, Z., Lee, D., Liousse, C., Mieville, A., Owen, B., Schultz, M. G., Shindell, D., Smith, S. J., Stehfest, E., Van Aardenne, J., Cooper, O. R., Kainuma, M., Mahowald, N., McConnell, J. R., Naik, V., Riahi, K., and van Vuuren, D. P.: Historical (1850–2000) gridded anthropogenic and biomass burning emissions of reactive gases and aerosols: methodology and application, Atmos. Chem. Phys., 10, 7017-7039, doi:10.5194/acp-10-7017-2010, 2010.

Lemke, P., J. Ren, R.B. Alley, I. Allison, J. Carrasco, G. Flato, Y. Fujii, G. Kaser, P. Mote, R.H. Thomas and T. Zhang: Observations: Changes in Snow, Ice and Frozen Ground. In: Climate Change 2007: The Physical Science Basis. Contribution of Working Group I to the Fourth Assessment Report of the Intergovernmental Panel on Climate Change [Solomon, S., D. Qin, M. Manning, Z. Chen, M. Marquis, K.B. Averyt, M. Tignor and H.L. Miller (eds.)]. Cambridge University Press, Cambridge, United Kingdom and New York, NY, USA, 2007.

Lohmann, U. and Feichter, J.: Global indirect effects: a review, *Atmos. Chem. Phys., 5, 715-737, 2005.*

Lubin, D. and A. M. Vogelmann: A climatologically significant aerosol longwave indirect effect in the Arctic. Nature, 439, 453-456, *2006.*

Marshall S, Oglesby RJ: An improved snow hydrology for GCMs. Part I: snow cover fraction, albedo, grain size, and age. Clim Dyn 10:21–37, 1994.

Ménégoz, M., Voldoire, A., Teyssèdre, H., Salas y Mélia, D., Peuch, V.-H., Gouttevin, I.: How does the atmospheric variability drive the aerosol residence time in the Arctic region?, Tellus B, 64, 11596, DOI: 10.3402, 2012.

Moss, R., Babiker, M., Brinkman, S., Calvo, E., Carter, T., Edmonds, J., Elgizouli, I., Emori, S., Erda, L., Hibbard, K., Jones, R., Kainuma, M., Kelleher, J., Lamarque, J.F., Manning, M., Matthews, B., Meehl, J., Meyer, L., Mitchell, J., Nakicenovic, N., O'Neill, B., Pichs, R., Riahi, K., Rose, S., Runci, P., Stouffer, R., van Vuuren, D., Weyant, J., Wilbanks, T., van Ypersele, J.P., and Zurek, M.: Towards New Scenarios for Analysis of Emissions, Climate Change, Impacts, and Response Strategies. Technical Summary. Intergovernmental Panel on Climate Change, Geneva, 25 pp. 2008.

Moss R.*H., Edmonds, J.A., Hibbard, K., Manning, M., Rose, S.K., Van Vuuren, R.D., Carter, T., Emori, S., Kainuma, M., Kram, T., Meehl, G., Mitchell, J., Nakicenovic, N., Riahi, K., Smith, S.J., Stouffer, R., Thomson, A.M., Weyant, J. and Wilbanks, T.: "The Next Generation of Scenarios for Climate Change Research and Assessment." Nature 463(7282):747-756. doi:10.1038/nature08823, 2010.*

Mote, P. W., Hamlet, A. F., *Clark, M. P. and Lettenmaier, D. P.: Declining mountain snowpack in western North America. Bull. Amer. Meteor. Soc., 86, 39–49, 2005.*

National Ice Center. 2008, updated daily. IMS daily Northern Hemisphere snow and ice analysis at 4 km and 24 km resolution. Boulder, CO: National Snow and *Ice Data Center. Digital media, 2008.*

Ohara, T., Akimoto, H., Kurokawa, J., Horii, N., Yamaji, K., Yan, X., and Hayasaka, T.: An Asian emission inventory of anthropogenic emission sources for the period 1980–2020, Atmos. Chem. Phys., 7, 4419-4444, doi:10.5194/acp-7-4419-2007, 2007.

Penner, J. E., Andreae, M., Annegarn, H., Barrie, L., Feichter, J., Hegg, D., Jayaraman, A., Leaitch, R., Murphy, D., Nganga, J., and Pitari, G.: Aerosols, their Direct and Indirect Effects, in: Climate Change 2001: The Scientific Basis (edited by: Houghton, J. T., Ding, Y., Griggs, D. J., Noguer, M., Van der Linden, P. J., Dai, X., Maskell, K., and Johnson, C. A.), Report to Intergovernmental Panel on Climate Change from the Scientific Assessment Working Group (WGI), Cambridge University Press, 289–416, 2001.

Peters, G. P., Nilssen, T. B., Lindholt, L., Eide, M. S., Glomsrød, S., Eide, L. I., and Fuglestvedt, J. S.: Future emissions from shipping and petroleum activities in the Arctic, Atmos. Chem. Phys., 11, 5305-5320, doi:10.5194/acp-11-5305-2011, 2011.

Qu X., Hall, A.: What controls the strength of snow albedo feedback? J. Clim. 20: 3971-3981, DOI:10.1175/JCLI4186.1, 2007.

Qu X., Hall, A.: Assessing snow albedo feedback in simulated climate change. J. Clim. 19: 2617-2630, 2006.

Quaas, J., Ming, Y., Menon, S., Takemura, T., Wang, M., Penner, J. E., Gettelman, A., Lohmann, U., Bellouin, N., Boucher, O., Sayer, A. M., Thomas, G. E., McComiskey, A., Feingold, G., Hoose, C., Kristjánsson, J. E., Liu, X., Balkanski, Y., Donner, L. J., Ginoux, P. A., Stier, P., Grandey, B., Feichter, J., Sednev, I., Bauer, S. E., Koch, D., Grainger, R. G., Kirkevåg, A., Iversen, T., Seland, Ø., Easter, R., Ghan, S. J., Rasch, P. J., Morrison, H., Lamarque, J.-F., Iacono, M. J., Kinne, S., and Schulz, M.: Aerosol indirect effects – general circulation model intercomparison and evaluation with satellite data, Atmos. Chem. Phys., 9, 8697-8717, doi:10.5194/acp-9-8697-2009, 2009.

Quinn, P.K., T.S. Bates, E. Baum, N. Doubleday, A. Fiore, M. Flanner, A. Fridlind, T. Garrett, D. Koch, S. Menon, D. Shindell, A. Stohl, and S.G. Warren, Short-lived pollutants in the Arctic: Their climate impact and possible mitigation strategies, Atmos. Chem. Phys., 8, 1723-1735, 2008.

Riahi, K., Gruebler, A. & Nakicenovic, N. Scenarios of long-term socio-economic and environmental development under climate stabilization. Technol. Forecast. Soc. Change 74, 887–35, 2007.

Rayner, N. A., Parker, D. E., Horton, E. B., Folland, C. K., Alexander, L. V., Rowell, D. P., Kent, E.C. and Kaplan, A.: Global analyses of sea surface temperature, sea ice, and night marine air temperature since the late nineteenth century, J. Geophys. Res., Vol. 108, No. D14, 4407 10.1029/2002JD002670, 2003.

Roesch, A.: Evaluation of surface albedo and snow cover in AR4 coupled climate models, J. Geophys. Res., 111, D15111, doi:10.1029/2005JD006473, 2006.

Roesch, A., M. Wild, and A. Ohmura, Snow cover fraction in a General Circulation Model, in Remote Sensing and Climate Modeling: Synergies and Limitations, edited by M. Beniston and M. M. Verstraete, pp. 203–232, Kluwer Acad., Norwell, Mass., 2001.

Serreze, M. C., and J. A. Francis: The arctic amplification debate. Climatic Change 76(3-4): 241-264, doi:1007/s10584-005-9017-y, 2006.

Serreze, M. C., M. M. Holland, and J. Stroeve: Perspectives on the Arctic's shrinking sea-ice cover. Science 315(5818): 1533-1536, 2007.

Shaw, G. E.: The Arctic haze phenomenon, B. Am. Meteorol. Soc., 76, 2403–2413, 1995.

Shi, X., Groisman, P. Ya., Déry, S. J., and Lettenmaier, D. P.: The role of surface energy fluxes in pan-Arctic snow cover changes, Env. Res. Lett., 6, 035204, 2011.

Shindell, D. T.: Evaluation of the absolute regional temperature potential, Atmos.Chem. Phys., 12, 7955-7960, doi:10.5194/acp-12-7955-2012, 2012.

Shindell, D. T., Chin, M., Dentener, F., Doherty, R. M., Faluvegi, G., Fiore, A. M., Hess, P., Koch, D. M., MacKenzie, I. A., Sanderson, M. G., Schultz, M. G., Schulz, M., Stevenson, D. S., Teich, H., Textor, C., Wild, O., Bergmann, D. J., Bey, I., Bian, H., Cuvelier, C., Duncan, B. N., Folberth, G., Horowitz, L. W., Jonson, J., Kaminski, J. W., Marmer, E., Park, R., Pringle, K. J., Schroeder, S., Szopa, S., Takemura, T., Zeng, G., Keating, T. J., and Zuber, A.: A multi-model assessment of pollution transport to the Arctic. Atmos. Chem. Phys., 8, 5353-5372, 2008.

Shindell, D.: Local and remote contributions to Arctic warming. Geophys. Res. Lett., 34, L14704, doi:10.1029/2007GL030221, 2007.

Shindell, D., G. Faluvegi, A. Lacis, J. Hansen, R. Ruedy, and E. Aguilar: Role of tropospheric ozone increases in 20th century climate change. J. Geophys. Res., 111, D08302, doi:10.1029/2005JD006348, 2006.

Shi, X., Groisman, P.Y., Déry, S. and Lettenmaier, D.P.: The role of surface energy fluxes in pan-Arctic snow cover changes Environ. Res. Lett. 6, 035204. 2011.

Stohl, A: Characteristics of atmospheric transport into the Arctic troposphere. J. Geophys. Res., 111, D11306., doi:10.1029/2005JD006888, 2006.

Smith, S. J., van Aardenne, J., Klimont, Z., Andres, R. J., Volke, A., and Delgado Arias, S.: Anthropogenic sulfur dioxide emissions: 1850–2005, Atmos. Chem. Phys., 11, 1101-1116, doi:10.5194/acp-11-1101-2011, 2011.

Søvde, O. A., Gauss, M., Isaksen, I. S. A., Pitari, G., and Marizy, C.: Aircraft pollution – a futuristic view, Atmos. Chem. Phys., 7, 3621-3632, doi:10.5194/acp-7-3621-2007, 2007.

Textor, C., Schulz, M., Guibert, S., Kinne, S., Balkanski, Y., Bauer, S., Berntsen, T., Berglen, T., Boucher, O., Chin, M., Dentener, F., Diehl, T., Easter, R., Feichter, H., Fillmore, D., Ghan, S., Ginoux, P., Gong, S., Grini, A., Hendricks, J., Horowitz, L., Huang, P., Isaksen, I., Iversen, I., Kloster, S., Koch, D., Kirkevag, A., Kristjansson, J. E., Krol, M., Lauer, A., Lamarque, J. F., Liu, X., Montanaro, V., Myhre, G., Penner, J., Pitari, G., Reddy, S., Seland, Ø., Stier, P., Takemura, T., and Tie, X.: Analysis and quantification of the diversities of aerosol life cycles within AeroCom. Atmos. Chem. Phys., 6, 1777–1813, 2006.

Textor, C., Schulz, M., Guibert, S., Kinne, S., Balkanski, Y., Bauer, S., Berntsen, T., Berglen, T., Boucher, O., Chin, M., Dentener, F., Diehl, T., Feichter, J., Fillmore, D., Ginoux, P., Gong, S., Grini, A., Hendricks, J., Horowitz, L., Huang, P., Isaksen, I. S. A., Iversen, T., Kloster, S., Koch, D., Kirkevåg, A., Kristjansson, J. E., Krol, M., Lauer, A., Lamarque, J. F., Liu, X., Montanaro, V., Myhre, G., Penner, J. E., Pitari, G., Reddy, M. S., Seland, Ø., Stier, P., Takemura, T., and Tie, X.: The effect of harmonized emissions on aerosol properties in global models – an AeroCom experiment. Atmos. Chem. Phys., 7, 4489-4501, 2007.

Wang, X., S. J. Doherty, and J. Huang (2012), Black carbon and other light-absorbing impurities in snow across Northern China, J. Geophys. Res., doi:10.1029/2012JD018291, in press.

Warneke, C.,Bahreini, R., Brioude, J., Brock, C.A., de Gouw, J.A., Fahey, D.W., Froyd, K.D., Holloway, J.S., Middlebrook, A., Miller, L., Montzka, S., Murphy, D.M., Peischl, J., Ryerson, T.B., Schwarz, J.P., Spackman, J.R. and Veres, P.: Biomass burning in Siberia and Kazakhstan as an important source for haze over the Alaskan Arctic in April 2008. Geophys. Res. Lett., 36, L02813, doi:10.1029/2008GL036194, 2009.

Wiscombe W., and Warren, S.: A model for the spectral albedo of snow II. Snow containing atmospheric aerosols J. Atmos. Sci.,, 37, 2734-2745, 1980.

Table 1: Period, aerosol emissions and description of the nudging protocol for our 8 simulations. (x2) in the period means that the simulation was performed a second time with a slightly modified initial conditions to get 20 years of simulation as 10 years would clearly be insufficient to make comparisons statistically robust. Note that all simulations were made with prescribed Sea Surface Temperature (SST, observed for present-day simulations, or simulated from a previous coupled ocean-atmosphere model simulation for future periods).

Simulation	Period	Emissions	Description
S1	1998-2008	Current	Horizontal wind nudged toward ECMWF
S1B	1998-2008	Current	Horizontal wind nudged toward ECMWF - No snow albedo change with aerosol deposition
S2	2049-2060 (x2)	IPCC – 2050	No nudging
S3	2049-2060 (x2)	IPCC – 2050 + increased Arctic ships	No nudging
S4	2049-2060 (x2)	IPCC – 2050 + increased biomass burning	No nudging
S2_N	2049-2060	IPCC - 2050	Horizontal wind nudged toward S2
S3_N	2049-2060	IPCC – 2050 + increased Arctic ships	Horizontal wind nudged toward S2
S4_N	2049-2060	IPCC – 2050 + increased biomass burning	Horizontal wind nudged toward S2

Figure captions:

Figure 1: Annual mean of BC emissions (mg m^{-2} $month^{-1}$); (a): Current emissions (S1, total=2878 Gg/yr); (b): difference between 2050 RCP8.5 scenario and current emissions (S2-S1; difference= -1588 Gg/yr); (c): difference in 2050 ships emissions in a scenario with a large ship traffic over the Arctic region (Corbett et al.; 2010) with the 2050 RCP8.5 projected ship traffic scenario (S3-S2, difference=+3.9 Gg/yr); (d): difference in 2050 fire emission between a scenario with lengthened biomass burning season (constructed after Flanningan et al. ; 2009a, 2009b) and the 2050 RCP8.5 scenario projected fire emissions (S4-S2, difference=+235.9 Gg/yr).

Figure 2: Mean number of days per year with snow at the surface (MNDWS); (a): present-day (1997-2008) observation from NSIDC; (b): present-day simulation with BC effects on snow albedo (S1); (c): RMSE between model and observation for the whole period 1998-2008.

Figure 3: Mean number of days per year with snow at the surface (MNDWS); (a):Present-day MNDWS difference induced by BC deposition on snow; S1-S1B. (b): MNDWS difference between 2050 climate with RCP8.5 emission scenario and present-day simulation (S2_N-S1); (c): MNDWS difference between a 2050 scenario with higher ship traffic in the Arctic in comparison with 2050 RCP8.5 scenario (S3_N-S2_N); (d): MNDWS difference between a 2050 scenario with increased biomass burning activity in comparison with 2050 RCP8.5 scenario (S4_N-S2_N). Note that future simulations are nudged toward the S2_N future simulation. Areas with statistically significant differences, according to a two-sample t-test, are shaded in grey. Note that the changes shown in (a) and (b) are statistically significant over the major part of the domain.

Figure 4: Mean number of days per year with snow at the surface (MNDWS); (a): MNDWS difference between a 2050 scenario with higher ship traffic in the Arctic in comparison with 2050 RCP8.5 scenario (S3-S2); (d): MNDWS difference between a 2050 scenario with increased biomass burning activity in comparison with 2050 RCP8.5 scenario (S4-S2). Simulations S2, S3 and S4 are not nudged. Areas with statistically significant differences, according to a two-sample t-test, are shaded in grey and contoured.

Figure 5: Spring (April-May-June) BC continental deposition (mg m^{-2} $month^{-1}$) ; (a): Present-day deposition (S1, total=222 Gg $month^{-1}$); (b): difference in deposition between RCP8.5 scenario for 2050 and present-day simulation (S2-S1, difference=-110 Gg $month^{-1}$); (c): difference in deposition between a 2050 scenario with enhanced ship traffic over the Arctic and an RCP8.5 scenario for 2050 (S3-S2, difference=-0.8 Gg $month^{-1}$); (d): difference in deposition between a scenario with increased biomass burning activity for 2050 and the RCP8.5 scenario for 2050 (S4-S3, difference=+21 Gg $month^{-1}$). Areas with statistically significant differences, according to a two-

sample t-test, appear in grey shading. Note that the changes shown in (b) and (c) are statistically significant over the major part of the domain.

Figure 6: Spring (April-May-June) average of snow depth (SWE, mm): (a) Present-day SWE, S1; (b): Present-day SWE difference induced by BC deposition on snow (S1-S1B), (c): Difference between 2050 RCP8.5 scenario and present-day SWE (S2-S1); (d): SWE difference in a 2050 scenario with high-level ships traffic in the Arctic in comparison with 2050 RCP8.5 scenario (S3-S2); (e): SWE difference in a 2050 scenario with increased biomass burning activity in comparison with 2050 RCP8.5 scenario (S4-S2). Simulations for the middle of the 21st century are not nudged. Areas with statistically significant differences, according to a two-sample t-test, appear in grey shading. Note that the changes shown in (b) and (c) are statistically significant over the major part of the domain.

Figure 7: Spring (April-May-June) snowfall (SWE, mm month^{-1}) ; (a) Current snowfall ; (b): Present-day snowfall difference induced by BC deposition on snow (S1-S1B), (c): difference between 2050 RCP8.5 scenario and present snowfall (S2-S1); (d): snowfall difference in a 2050 scenario with high-level ships traffic in the Arctic in comparison with 2050 RCP8.5 scenario (S3-S2); (e): snowfall difference in a 2050 scenario with increased biomass burning activity in comparison with 2050 RCP8.5 scenario (S4-S2). Simulations for the middle of the 21st century are not nudged. Areas with statistically significant differences, according a two-sample t-test, appear in grey shading. Note that the changes shown in (b) and (c) are statistically significant over the major part of the domain.

Figures:

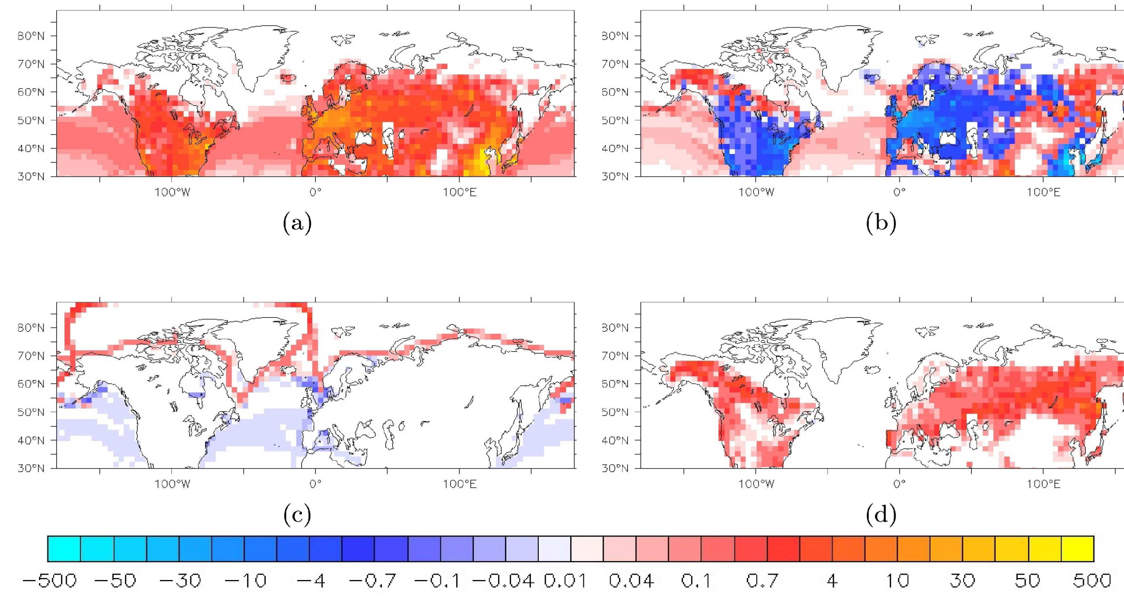

Figure 1: Annual mean of BC emissions (mg m^{-2} month^{-1}); (a): Current emissions (S1, total=2878 Gg/yr); (b): difference between 2050 RCP8.5 scenario and current emissions (S2-S1; difference= -1588 Gg/yr); (c): difference in 2050 ships emissions in a scenario with a large ship traffic over the Arctic region (Corbett et al.; 2010) with the 2050 RCP8.5 projected ship traffic scenario (S3-S2, difference=+3.9 Gg/yr); (d): difference in 2050 fire emission between a scenario with lengthened biomass burning season (constructed after Flanningan et al. ; 2009a, 2009b) and the 2050 RCP8.5 scenario projected fire emissions (S4-S2, difference=+235.9 Gg/yr).

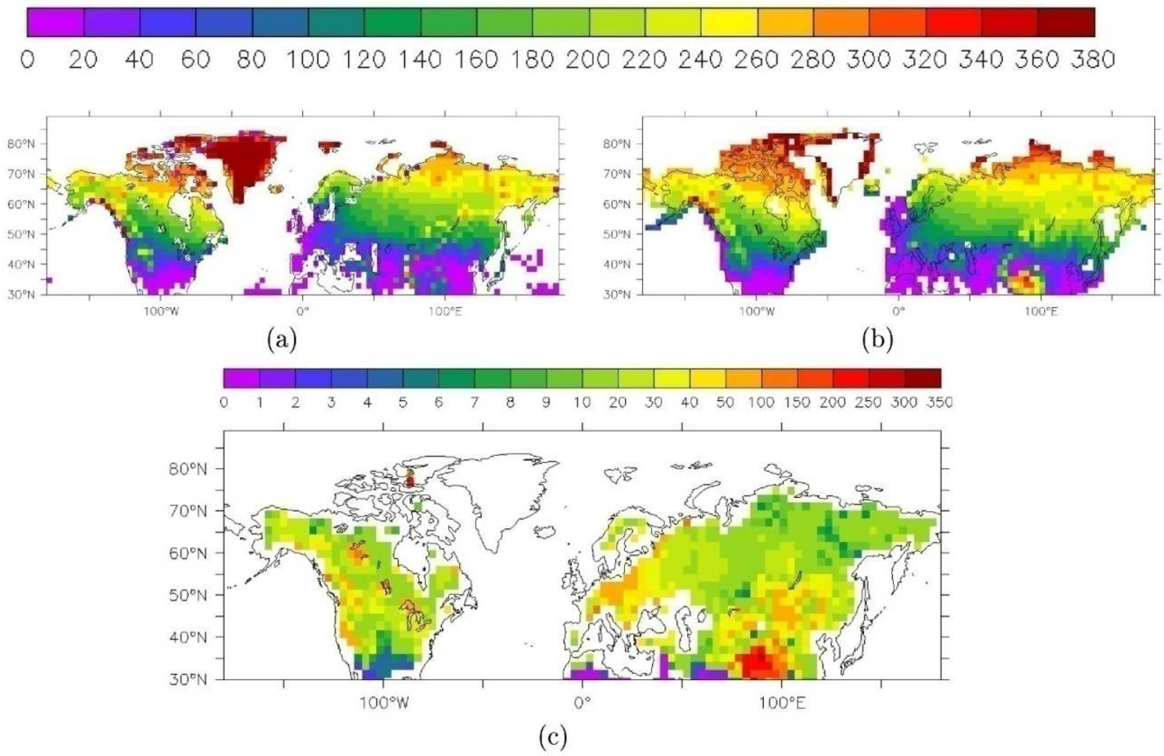

Figure 2: Mean number of days per year with snow at the surface (MNDWS); (a): present-day (1997-2008) observation from NSIDC; (b): present-day simulation with BC effects on snow albedo (S1); (c): RMSE between model and observation for the whole period 1998-2008.

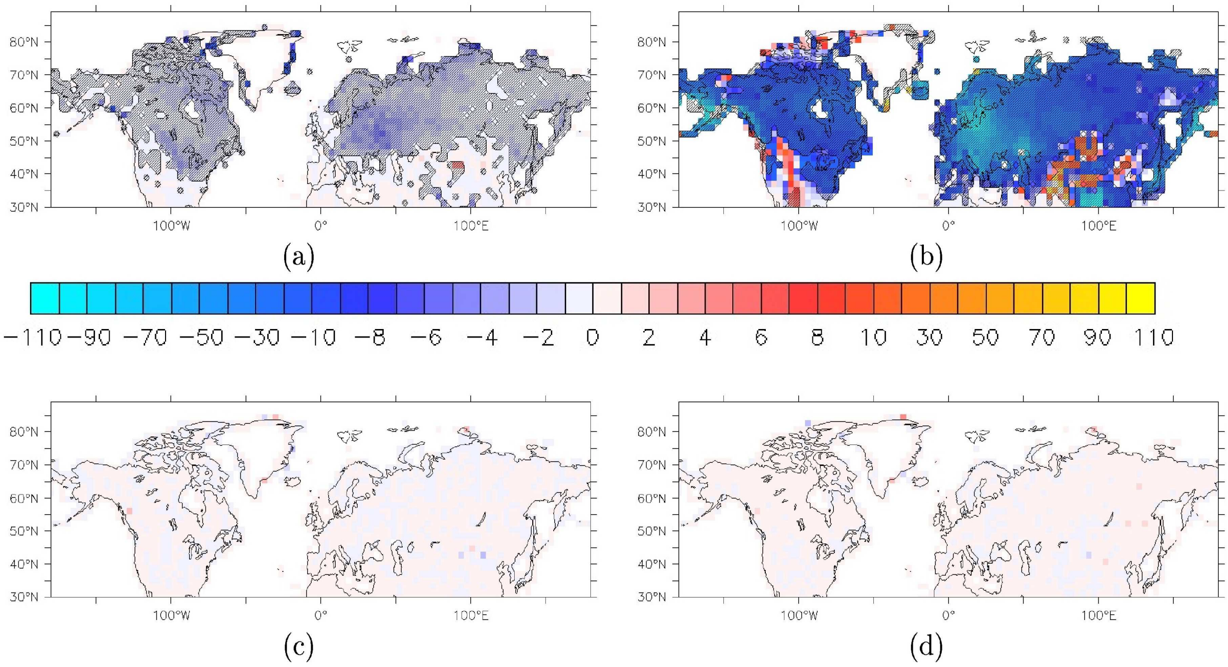

Figure 3: Mean number of days per year with snow at the surface (MNDWS); (a):Present-day MNDWS difference induced by BC deposition on snow; S1-S1B. (b): MNDWS difference between 2050 climate with RCP8.5 emission scenario and present-day simulation (S2_N-S1); (c): MNDWS difference between a 2050 scenario with higher ship traffic in the Arctic in comparison with 2050 RCP8.5 scenario (S3_N-S2_N); (d): MNDWS difference between a 2050 scenario with increased biomass burning activity in comparison with 2050 RCP8.5 scenario (S4_N-S2_N). Note that future simulations are nudged toward the S2_N future simulation. Areas with statistically significant differences, according to a two-sample t-test, are shaded in grey. Note that the changes shown in (a) and (b) are statistically significant over the major part of the domain.

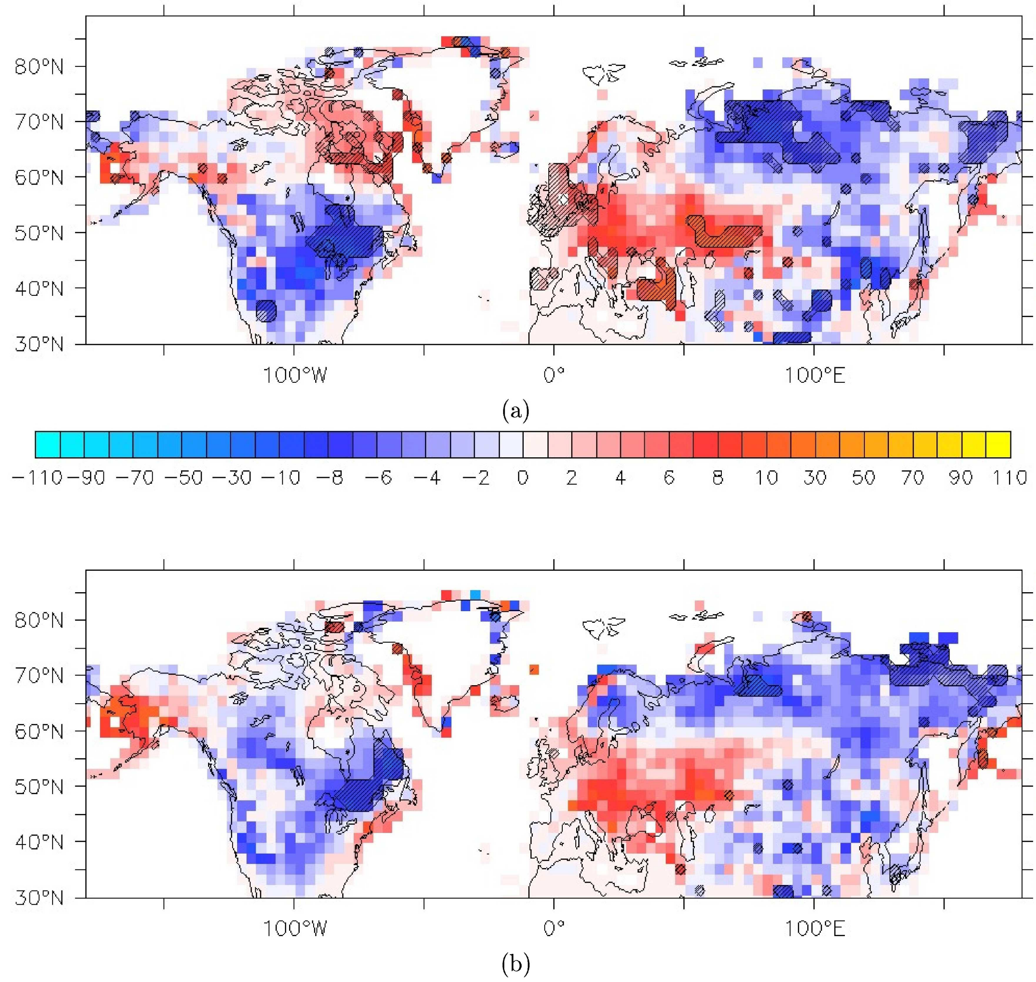

Figure 4: Mean number of days per year with snow at the surface (MNDWS); (a): MNDWS difference between a 2050 scenario with higher ship traffic in the Arctic in comparison with 2050 RCP8.5 scenario (S3-S2); (d): MNDWS difference between a 2050 scenario with increased biomass burning activity in comparison with 2050 RCP8.5 scenario (S4-S2). Simulations S2, S3 and S4 are not nudged. Areas with statistically significant differences, according to a two-sample t-test, are shaded in grey and contoured.

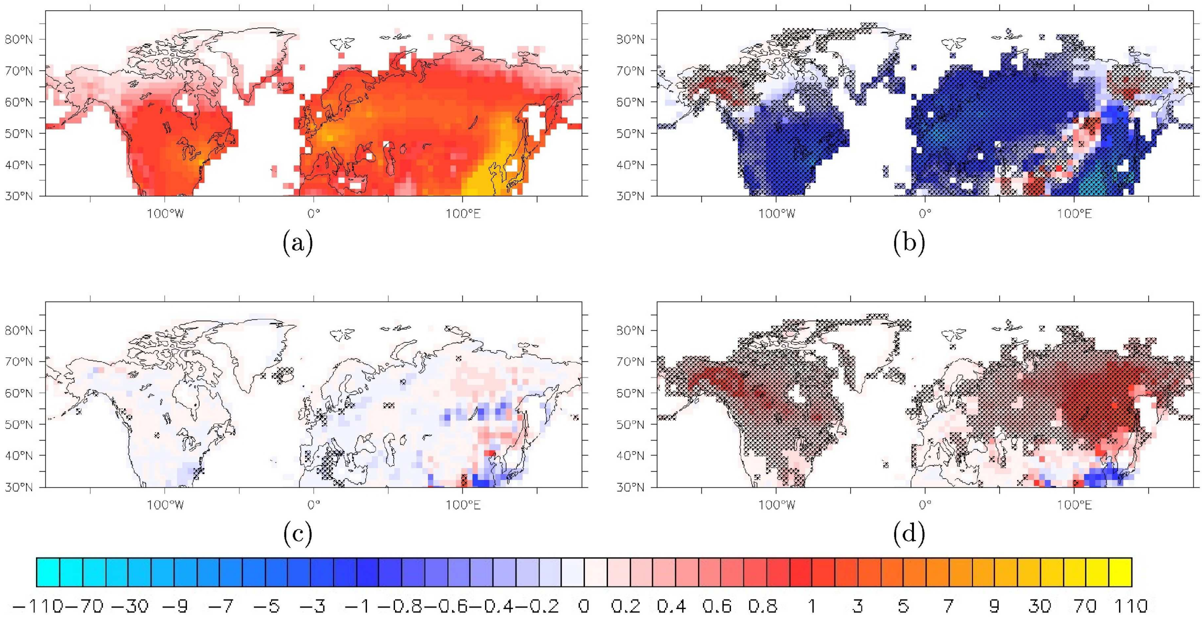

Figure 5: Spring (April-May-June) BC continental deposition (mg m^{-2} $month^{-1}$) ; (a): Present-day deposition (S1, total=222 Gg $month^{-1}$); (b): difference in deposition between RCP8.5 scenario for 2050 and present-day simulation (S2-S1, difference=-110 Gg $month^{-1}$); (c): difference in deposition between a 2050 scenario with enhanced ship traffic over the Arctic and an RCP8.5 scenario for 2050 (S3-S2, difference=-0.8 Gg $month^{-1}$); (d): difference in deposition between a scenario with increased biomass burning activity for 2050 and the RCP8.5 scenario for 2050 (S4-S3, difference=+21 Gg $month^{-1}$). Areas with statistically significant differences, according to a two-sample t-test, appear in grey shading. Note that the changes shown in (b) and (c) are statistically significant over the major part of the domain.

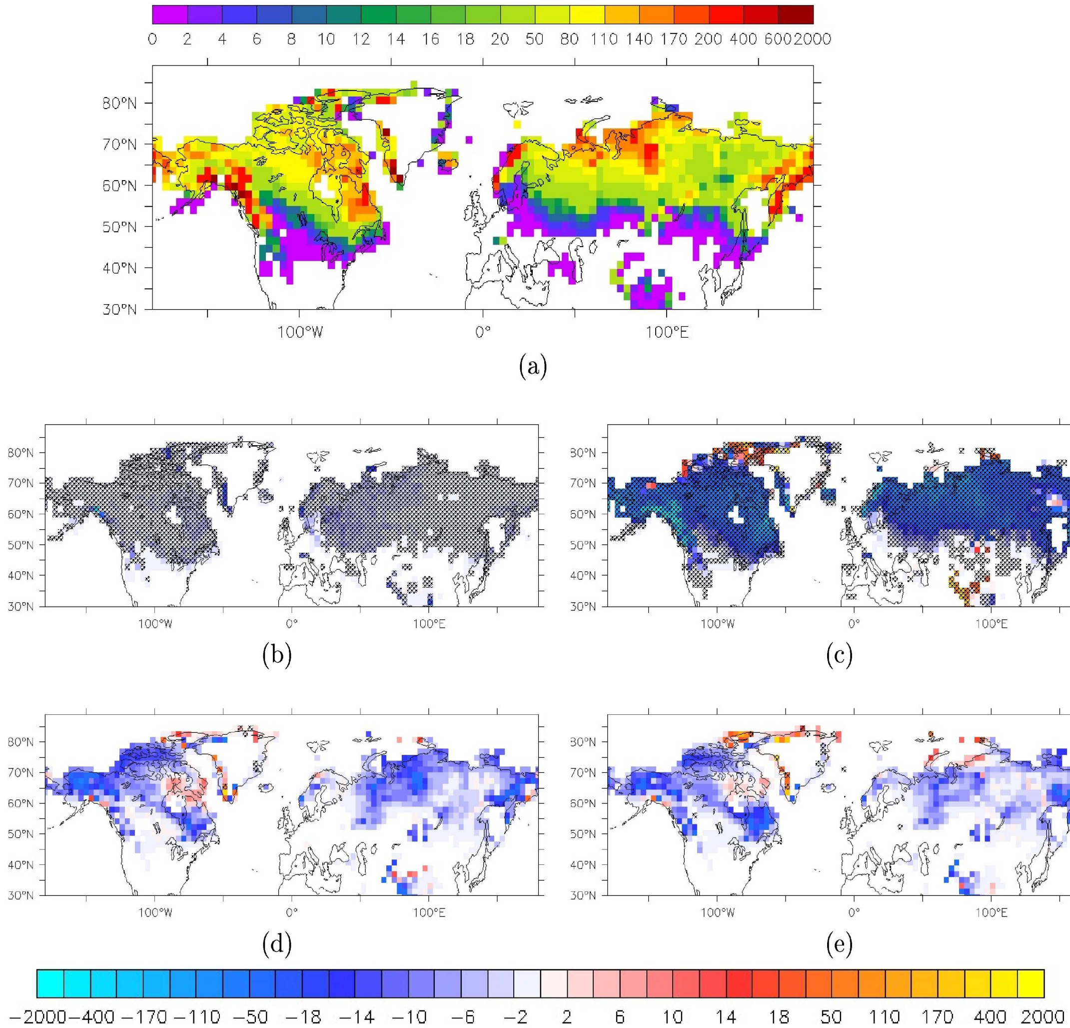

Figure 6: Spring (April-May-June) average of snow depth (SWE, mm): (a) Present-day SWE, S1; (b): Present-day SWE difference induced by BC deposition on snow (S1-S1B), (c): Difference between 2050 RCP8.5 scenario and present-day SWE (S2-S1); (d): SWE difference in a 2050 scenario with high-level ships traffic in the Arctic in comparison with 2050 RCP8.5 scenario (S3-S2); (e): SWE difference in a 2050 scenario with increased biomass burning activity in comparison with 2050 RCP8.5 scenario (S4-S2). Simulations for the middle of the 21st century are not nudged. Areas with statistically significant differences, according to a two-sample t-test, appear in grey shading. Note that the changes shown in (b) and (c) are statistically significant over the major part of the domain.

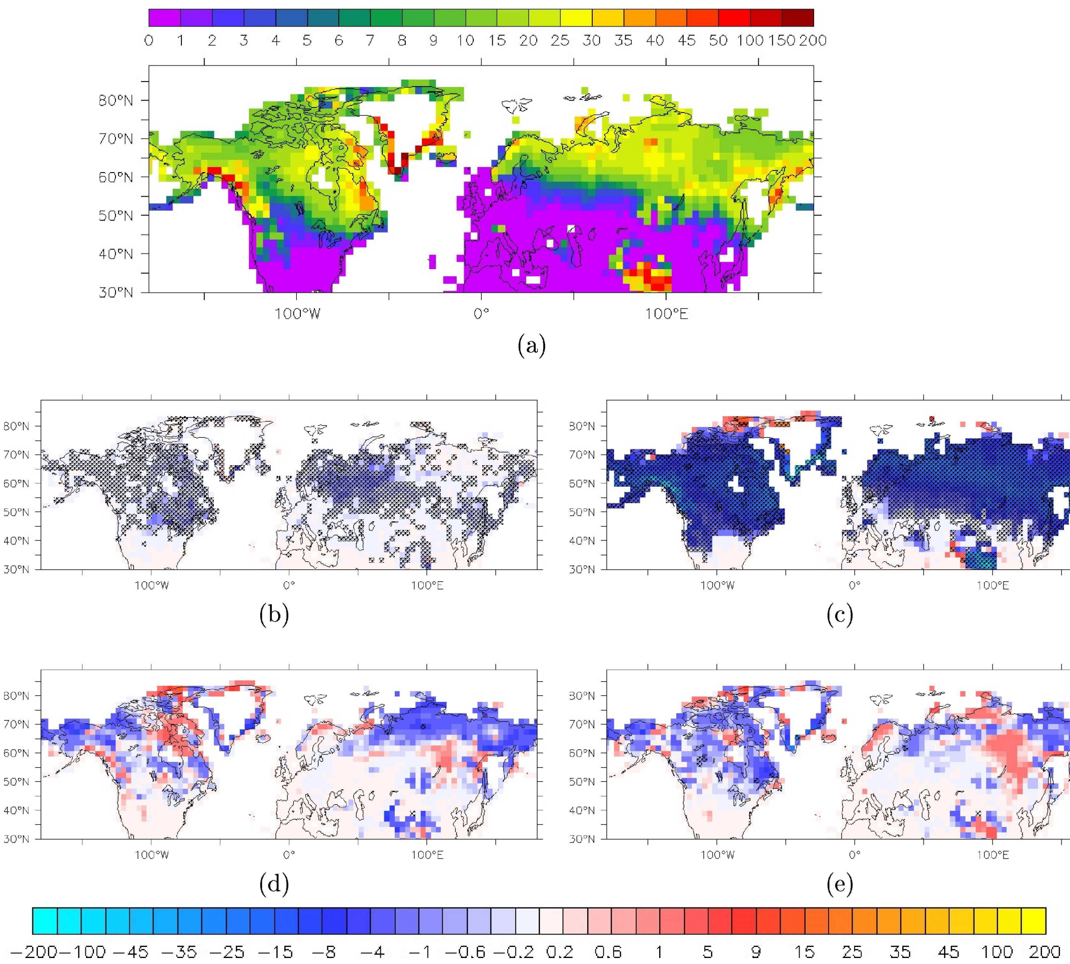

Figure 7: Spring (April-May-June) snowfall (SWE, mm month^{-1}) ; (a) Current snowfall ; (b): Present-day snowfall difference induced by BC deposition on snow (S1-S1B), (c): difference between 2050 RCP8.5 scenario and present snowfall (S2-S1); (d): snowfall difference in a 2050 scenario with high-level ships traffic in the Arctic in comparison with 2050 RCP8.5 scenario (S3-S2); (e): snowfall difference in a 2050 scenario with increased biomass burning activity in comparison with 2050 RCP8.5 scenario (S4-S2). Simulations for the middle of the 21st century are not nudged. Areas with statistically significant differences, according a two-sample t-test, appear in grey shading. Note that the changes shown in (b) and (c) are statistically significant over the major part of the domain.